Cryopreservation of the Kidney: A Feasibility Study Based on Cooling Rates

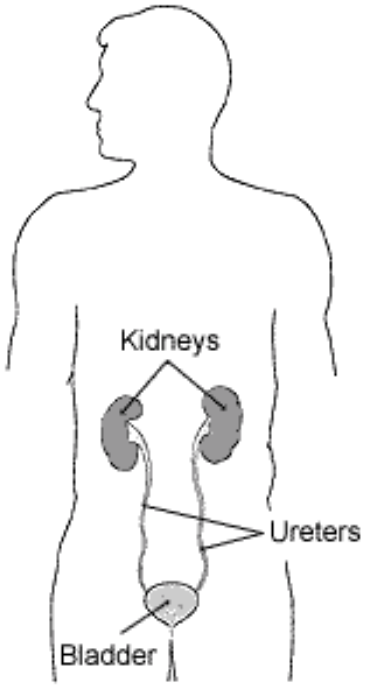

Erica Malvica
Ben Salter
Kush Verma
Tara Watkins
Michael Shauhgnesy
Bee 453
5-5-03

Executive Summary

This project models the cryopreservation of a kidney submerged in liquid nitrogen. Attempts to cryopreserve whole organs have been unsuccessful in the past due to the formation of ice crystals in the intracellular fluid, which cause damage to the cells. Damage can be avoided if cells are vitrified, which causes the intracellular fluid to form a glassy solid rather than ice crystals. The vitrification process is hard to achieve because it generally requires very high cooling rates, but it is aided by the addition of cryoprotectants. This study used Gambit ™ and Fidap™ software to model cooling rates using different concentrations of glycerol as a cryoprotectant. The concentrations of glycerol were varied to maximize vitrification, and thus cell survival. The results of this study show that the addition of cryoprotectant does alter the cooling rate. Cells closest to the surface of the kidney would likely have been vitrified while cells closer to the center had a slower cooling rate and would most likely have formed ice crystals. Cell survival is predicted to be highest for the 2M concentration of glycerol; however, higher concentrations should be avoided to prevent cell toxicity.

Introduction

Given recent advances in tissue engineering, the possibility of bioengineered tissues and organs becomes increasingly likely, and a potential method of storing these products becomes necessary. Current research in cryopreservation has resulted in reliable protocols for the freezing of cells and short-term (approximately 1 hr) preservation of tissues. The preservation of organs has been slowed by difficulties caused by the formation of ice inside the tissue; the formation of ice crystals not only creates obvious mechanical constraints on the cells, but also dramatically changes the concentration of the extracellular solution, which is normally carefully regulated by the cells. Recent research has developed a method of cryopreservation that prevents ice crystal formulation: vitrification. Vitrification involves the addition of a cryoprotectant which, when supercooled, causes the cell solution to form a glassy solid, which is less damaging to the cells.

Although this method is promising for the field of cryopreservation, there are several drawbacks. One of the major issues is the fact that the water must be removed from the tissues and replaced by a solution containing cryoprotectant at some concentration. Higher concentrations of cryoprotectant favour the vitrification process; unfortunately, many studies have found cryoprotectants to be toxic, and they must therefore be removed before use of the tissue or organ, or present only in dilute quantities. The other major issue is the supercooling required to cause vitrification. Vitrification will only occur at very rapid cooling rates; such rapid rates are usually achieved by immersing the object in liquid nitrogen. This method has proved successful for objects with small masses (such as red blood cells), but difficulties have been encountered with larger tissues and organs. The cooling rate at the centre of an organ is dependent on the thermal conductive properties of the surrounding tissues. Higher cooling rates are also favoured on the outer tissue layers, making it difficult to obtain the necessary cooling rates for vitrification at the centre of the organ.

Although the optimum cooling rates for cells seems to depend somewhat on the cell type, numerous research projects have been performed to determine general optimal cooling rates for maximum tissue cell survival. This project will utilise these cooling rates to determine the potential viability of a kidney submerged in liquid nitrogen. The

vitrification/freezing process of the kidney (with an added cryoprotectant) will be modelled in Fidap, and time/temperature data at various selected nodes will be used to reconstruct the cooling rates at various points through the kidney. The calculated cooling rates will then be compared with the optimal cooling rates to predict the cell survival rates in the kidney, and thus used to evaluate the potential success for vitrification of the kidney in this fashion.

The length of the kidney in the adult male averages 10 to 12 cm; its breadth is about 5 to 6 cm, and its thickness 3 to 4 cm. Its average weight is 160-170 g. The kidney model developed for this project (see Appendix A) is one-half a kidney at 10x5x1.75 cm, and is represented through a non-graded custom mesh. A schematic of the problem is shown below in Figure 1.

Figure 1: Problem Schematic

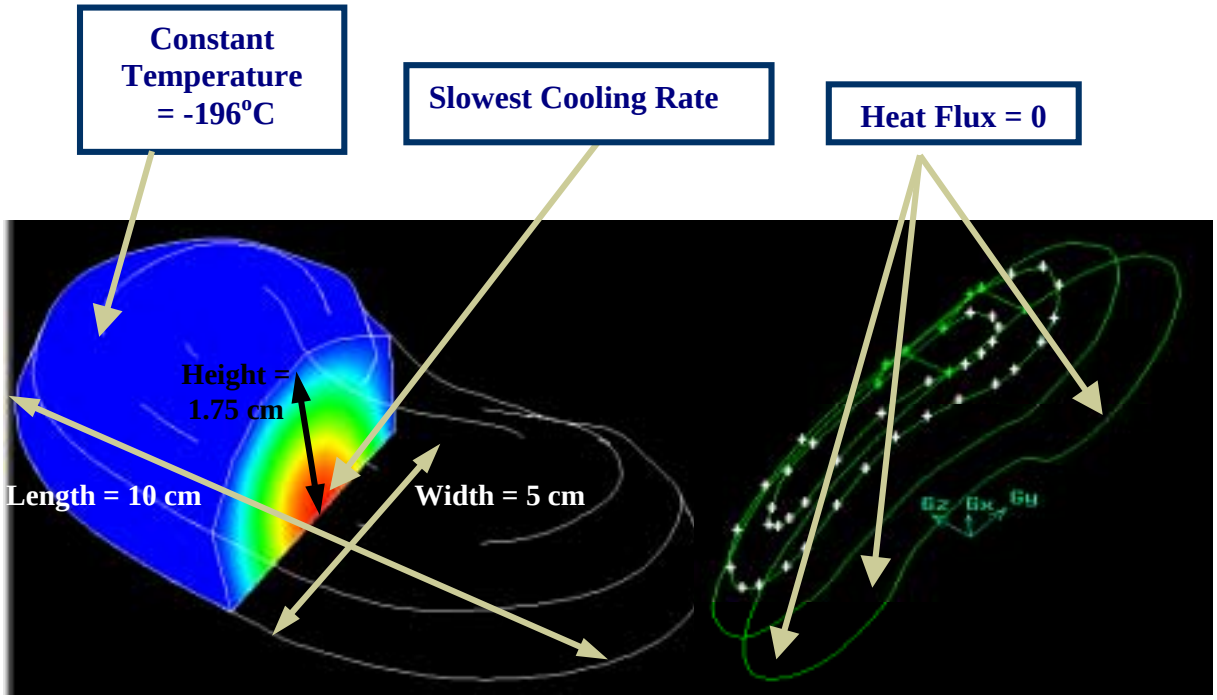

Cooling of the kidney tissues was modelled using the heat transfer equation, with the outer surface kept at a constant -196˚C. Theoretically, the outer surface is cooled by convection, but the heat transfer coefficient of liquid nitrogen is high enough that the surface can be considered constant at -196˚C. The kidney was assumed to be initially at body temperature (37˚C). The bisected face of the kidney (the interior face) has a heat

flux of zero, due to symmetry. Material properties used for initial calculations are as follows:

Thermal conductivity: 5.06 $*10^{-3}$ W/cm C
Density: 9.99 $*10^{-4}$ kg/cm^3
Specific heat: Assume water property = 4200 J/kg K

The above listed properties are only estimates of the true values. To refine the results, it was assumed that the enthalpy of frozen kidney tissue could be approximated by the enthalpy of frozen beef. Data from Mott (1964), on the variation of enthalpy in frozen beef with temperature, was used to calculate apparent specific heat values using the equation: $\Delta H/\Delta T = C_{p,a}$. The varying specific heat values were entered into Fidap™ to obtain results for the freezing rates of the kidney without any cryoprotectants. Specific heat was estimated (table 1 appendix A) from a range of temperature and enthalpy values.

Data on the variation of apparent specific heat of tissue with temperature in the presence of varying concentrations of cryoprotectant was not readily available, so specific heat values were calculated by estimating the enthalpy change from the following formula:

$$\Delta H = [(1-w)C_{p,s} + w*[[(1-f)*C_{p,w}+f*C_{p,i}]]* \Delta T - \lambda* \Delta f *w$$

Where:

$C_{p,i}$ = specific heat of ice = 2.09kJ/kg*C
$C_{p,w}$ = specific heat of water = 4.196 KJ/kg *C
$C_{p,s}$ = specific heat of solid matrix= .462 kJ/kg*C
w = fraction of tissue composed of water = 0.75
f = water fraction (water /ice)
λ = heat of fusion of water = 336 kJ/kg

To begin calculations, initial values for enthalpy, water fraction, and specific heat were arbitrarily set at 0. Water fractions at the various glycerol concentrations were obtained from a chart of unfrozen water fraction vs. temperature at various glycerol concentrations (Mazur, 1984). The water fraction was assumed to be 1 (solid phase only) until a notable change in water fraction could be approximated from the curves. These fractions were used in the above equation to find the change in enthalpy. The enthalpy change was added to the previous enthalpy value to determine the new value. Above freezing, the water fraction was assumed to be 0 (no water remained in solid form). The apparent specific heat at that temperature could then be calculated as previously, using

$\Delta H/\Delta T = C_{p,a}$. The resulting tables of values for 0.5 Molar glycerol and 2.0 Molar glycerol are given in Tables 2 and 3 in appendix A. These values, along with the original data on variation of enthalpy with temperature, were used to generate Figure 2. Only relevant values in the range of the temperature change were used in Fidap; specific heat values below –60˚C were assumed to be constant and equal to the enthalpy at –60˚C.

All the specific heat values peak in the range of phase change. Without cryoprotectant, the specific heat peaks at 84 kJ/Kg C; the addition of cryoprotectant causes a more gradual rise in the specific heat, leading to increased specific heat values over a wider temperature range, but a much lower maximum specific heat than without the addition of cryoprotectant, thus maintaining the same area under each curve.

Figure 2: Apparent Specific Heat at 0M, 0.5M and 2.0M Glycerol

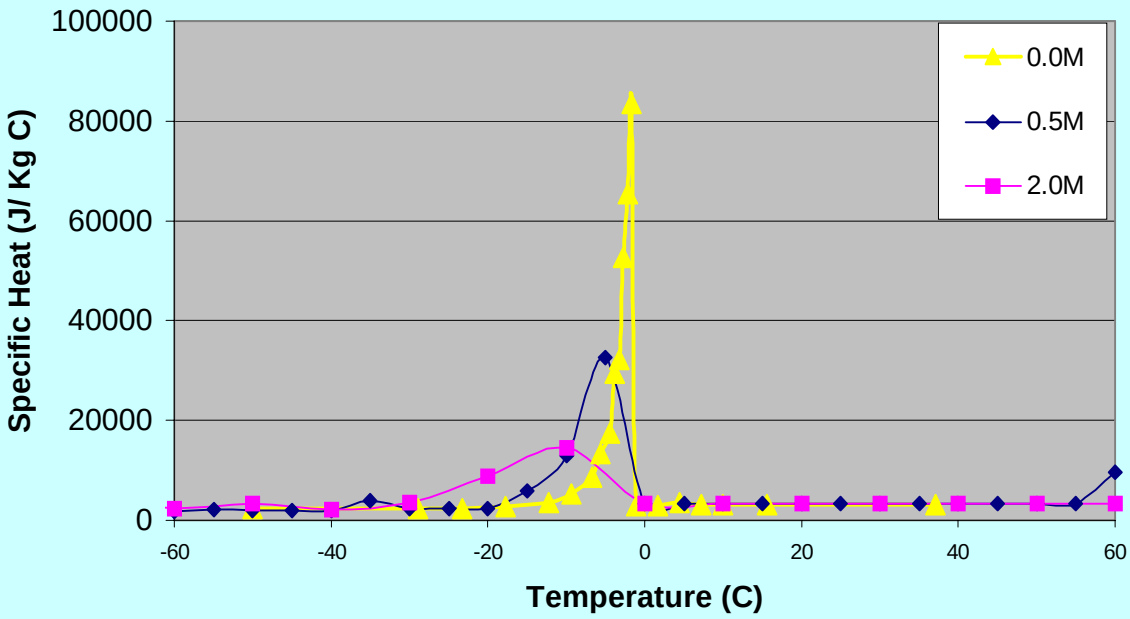

Design Objectives

The main objective of this project is to determine if sufficient cooling rates to achieve vitrification (and thus cell survival) can be obtained by adding the cryoprotectant glycerol to a kidney. The effects of cooling without cryoprotectant and at differing concentrations of gycerol will be examined to determine its effects on cooling rates in the tissue.

Results and Discussion

Analysis of Predicted Cell Survival Rates

Initial solutions of kidney freezing with 2M cryoprotectant are shown in the following contour graphs; figures 3-6 at time 0.1, 250, 500, and 700 seconds respectively.

Figure 3: Temperature Contours at 0.1 Seconds

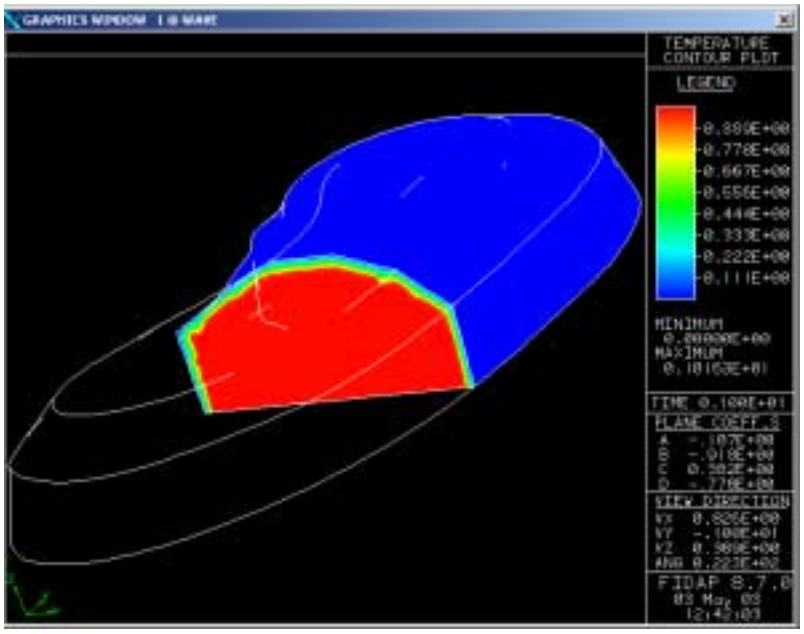

Figure 4: Temperature Contours at 250 seconds

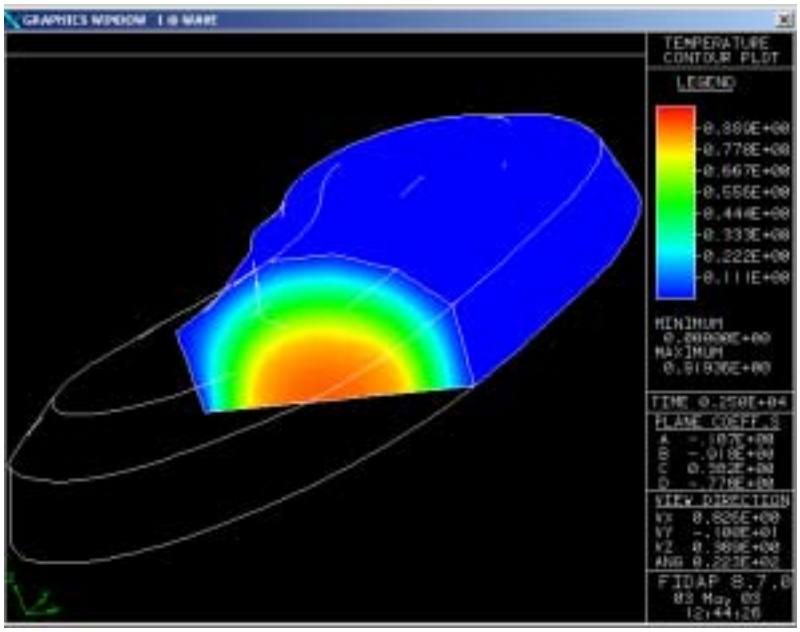

Figure 5: Temperature Contours at 500 seconds

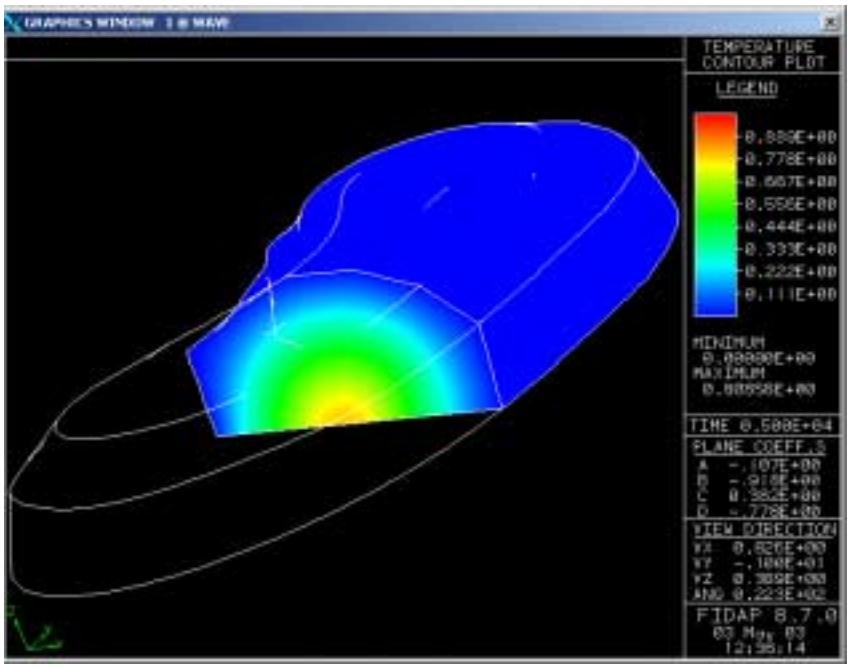

Figure 6: Temperature Contours at 700 seconds

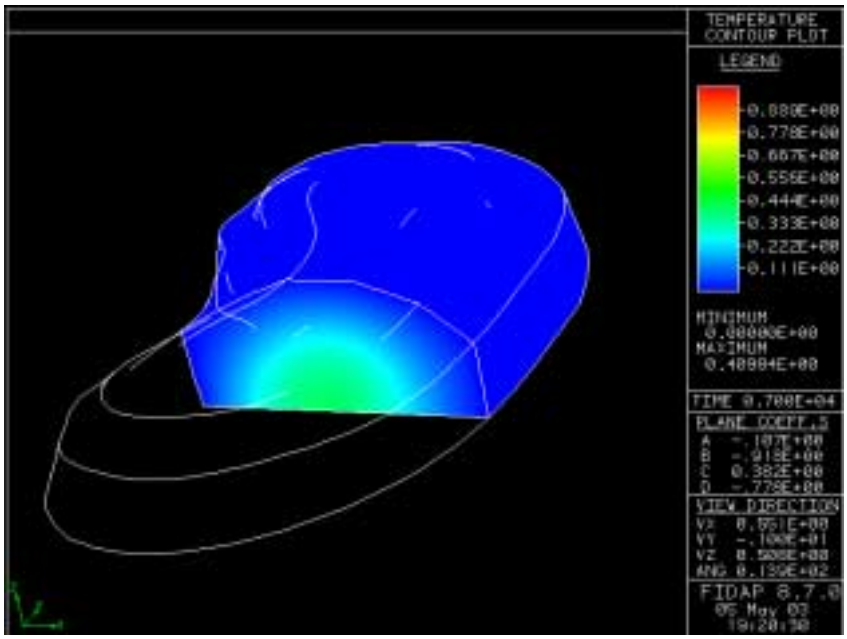

After 500 seconds, the temperature at the centre of the kidney has only just reached freezing, and only changes drastically after 500 seconds (Figure 7, below).

Figure 7: Temperature Vs. Time at the Center of the Kidney with 2.0 M Glycerol

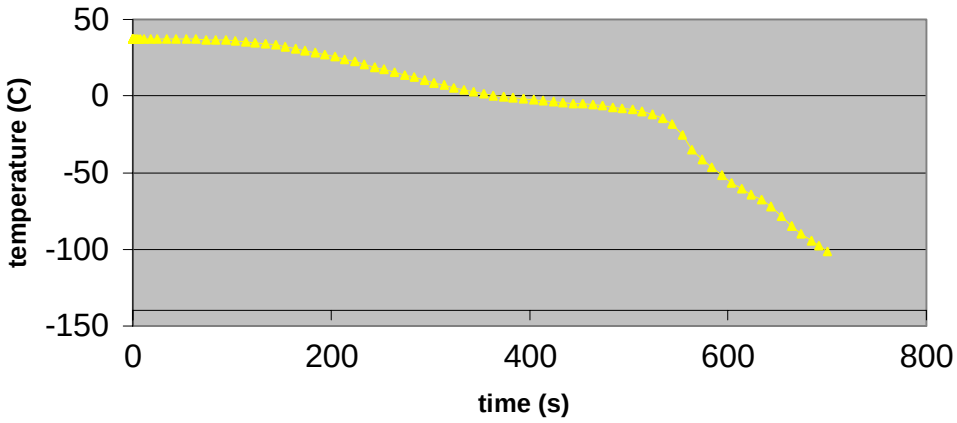

This slow change in temperature is due to the low conductivity of tissue, and indicates that cooling rates at the center will be too slow to induce vitrification. Although the cooling rates do increase significantly after 500 seconds of cooling, the rapid change in temperature appears to occur only after the centre has reached the freezing point, indicating that ice crystals would already have formed. Even if the increase in cooling rate occurred earlier in the cooling process, research on cell survival percentages with varying cooling rates indicates that at 2.0 M concentration of glycerol, a cooling rate of –1.7 C/s would be required for an 80% cell survival rate (Mazur, 1984), and this model predicts a maximum cooling rate of approximately –0.95 C/s (see Figure 8 below for cooling rates with time), with an estimated cell survival percentage of only 60%.

Figure 8: Cooling Rate vs. Time at the Center of the Kidney with 2.0 M Glycerol

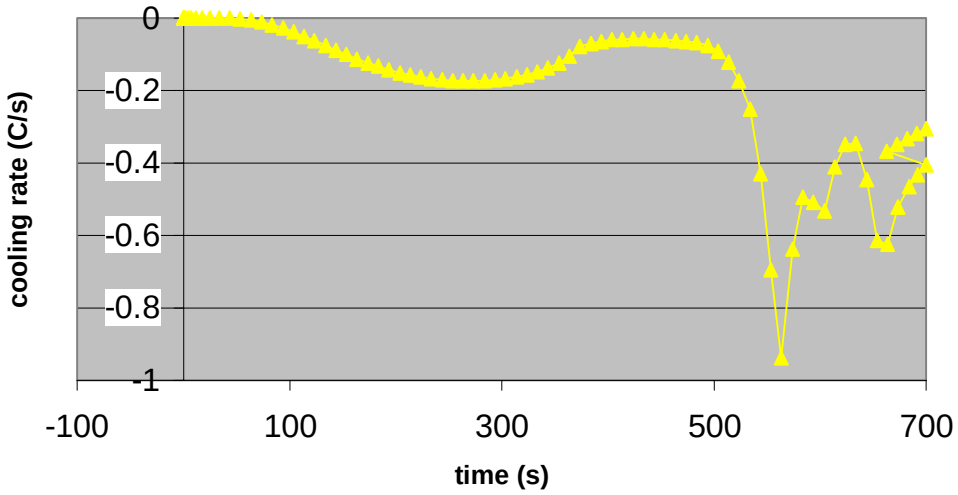

Hence, we can expect poor cell survival rates in the medulla. Faster cooling rates at or near the surface of the kidney, apparent in the contour plots shown in Figures 3-6 indicate better cell survival in the cortex. More specifically, we can expect damage to the loop of henle and the collecting duct of the nephrons. This damage will certainly prevent normal kidney function.

Comparison of the Effects of Cryoprotectant Concentrations

Analysis of the effect of glycerol concentration was based on the temperature change data at two nodes. Node 12500 is located halfway between the outer surface and the bisected inner half. Node 3942 is located at the middle of bisection, representing the center of the kidney. Figure 9, below, graphically illustrates the location of these two nodes.

Figure 9: Location of Nodes Used in Analysis

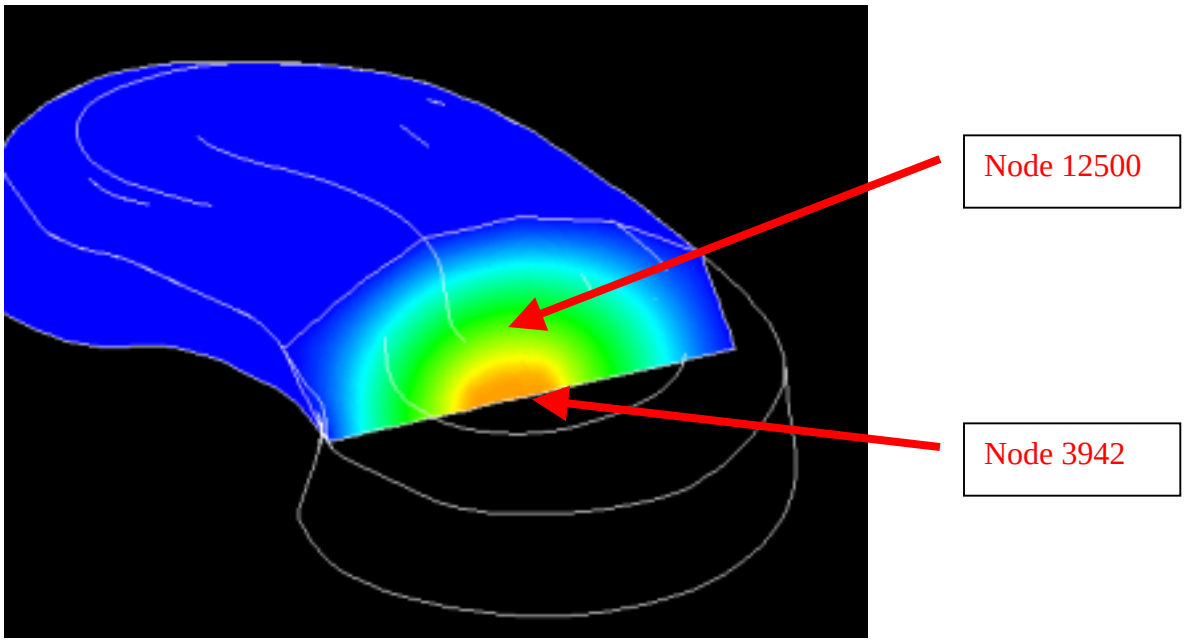

The cooling rates at both nodes were calculated over the entire cooling time (700 s) for each different concentration of glycerol. Graphs of the cooling rates with time at Node 3942 (the centre of the kidney) are shown in Figure 10, below, for each of the three glycerol concentrations (0 M or no glycerol, 0.5 M, and 2.0 M), and also includes the cooling rates with time for the model using a constant specific heat value. The model using a constant specific heat does not account for the affects of freezing and the latent heat of fusion in the phase change; the drastic effects of the change in specific heat with temperature are apparent in the other three graphs, which all have spikes in the cooling rates after 500 seconds. Before 500 seconds, the cooling rates could be modelled relatively accurately with a constant specific heat value, but as the temperature drops, the change in specific heat must necessarily be accounted for, and the model using a constant specific heat was determined to be inaccurate and inappropriate for this project. Thus, the following analysis includes only the models using varying specific heats. Not surprisingly, it can be observed from the graph that as higher concentrations of cryoprotectant are added, the cooling rate profile appears to more closely approach the

constant specific heat profile; this data agrees with the specific heat curves (Figure 2), which show more constant specific heats for higher concentrations of cryoprotectant.

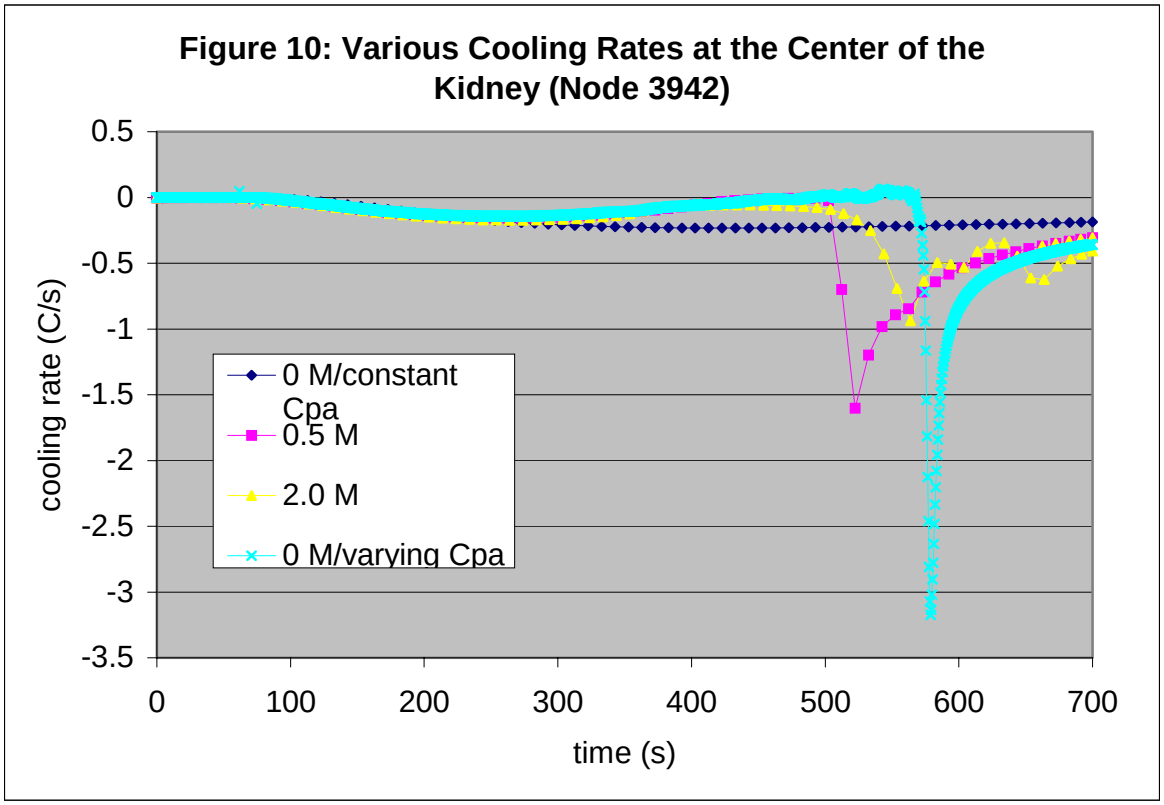

The apparent specific heat increases dramatically after the freezing point because the intercellular fluid is undergoing a liquid to solid phase change (Figure 2); thus, the specific heat will also drop dramatically following the phase change. Misleadingly, our results for the center of the kidney seem to indicate that the cooling rates are proportional to the specific heat, with cooing rates increasing at approximately the time of phase change. However, examination of the other node, located nearer the surface of the kidney, shows cooling rate peaks that are no longer proportional to the specific heats, indicating that the change in specific heat is not the cause of the peak in cooling rates.

In fact, examination of the graph indicates that in most cases, the cooling rate peak actually occurs shortly after the specific heat peak, that is, shortly after the phase change occurs. This fact is confirmed by comparing the temperature at which the

specific heat peaks occur (approximately -2.5, -5 , and –10 C respectively for 0, 0.5, and 2.0 M glycerol) with a graph of temperature vs. time for the center node (Figure 11) which indicates that these temperatures correspond to times of approximately 575, 500, and 500 seconds for the respective glycerol concentrations. Thus, since the cooling rate peaks occur at approximately 590, 575, and 525 seconds, all of the cooling rate peaks occur after the phase changes.

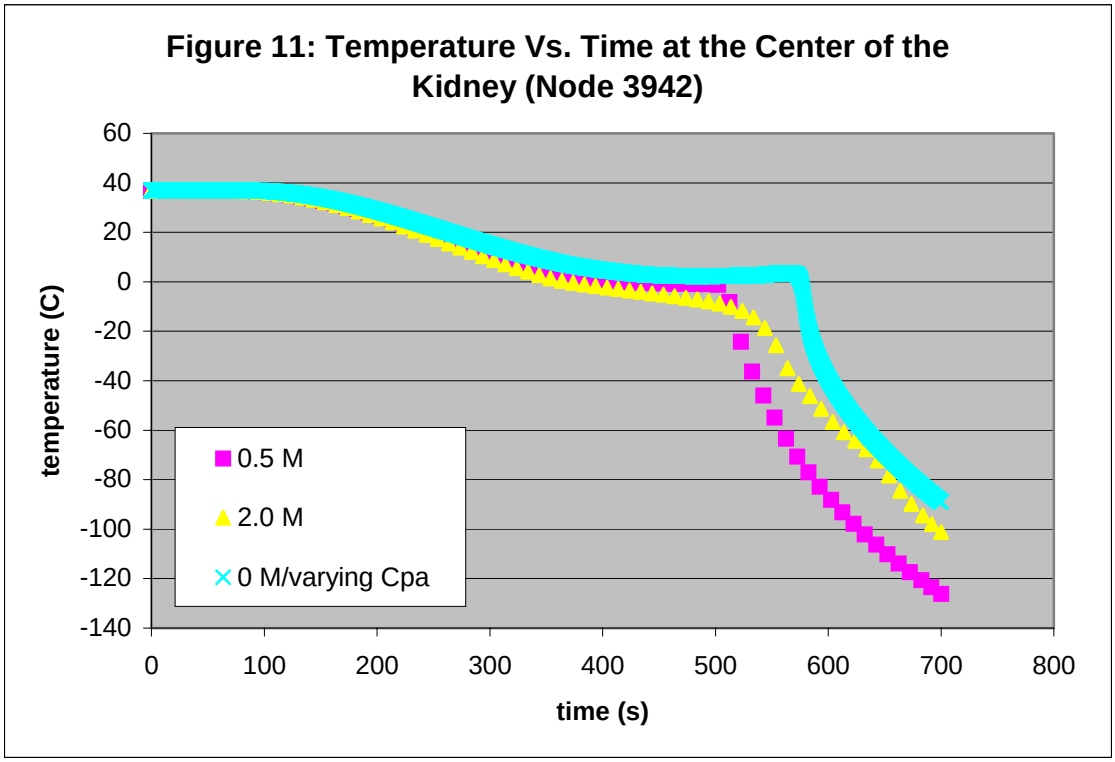

Thus, it seems that the peak in cooling rate at the center is more likely due to the semi-radial geometry of the kidney; the cells at the center only begin cooling quickly after the surrounding cells reach the phase change point, after which the decreased specific heat allows for more effective conduction of heat away from the center cells. . Since the kidney is largely radial, the cells surrounding the center node will reach phase change nearly simultaneously, resulting in rapid conduction of heat away from the center at all sides.

Since the addition of cryoprotectant alters the phase change somewhat (such that the intracellular fluid does not actually become a crystalline solid, but a highly viscous glassy solid), creating more uniform specific heats, the drop in specific heat following the phase change is not as drastic, producing a less drastic jump in the cooling rates. Instead,

the cooling rates with added cryoprotectant are somewhat lower for most of the cooling process, and actually yield lower temperatures at the end of the 700 s cooling period. A similar affect can be seen in Figure 12, below, for node 12500, which is between the center of the kidney and the surface.

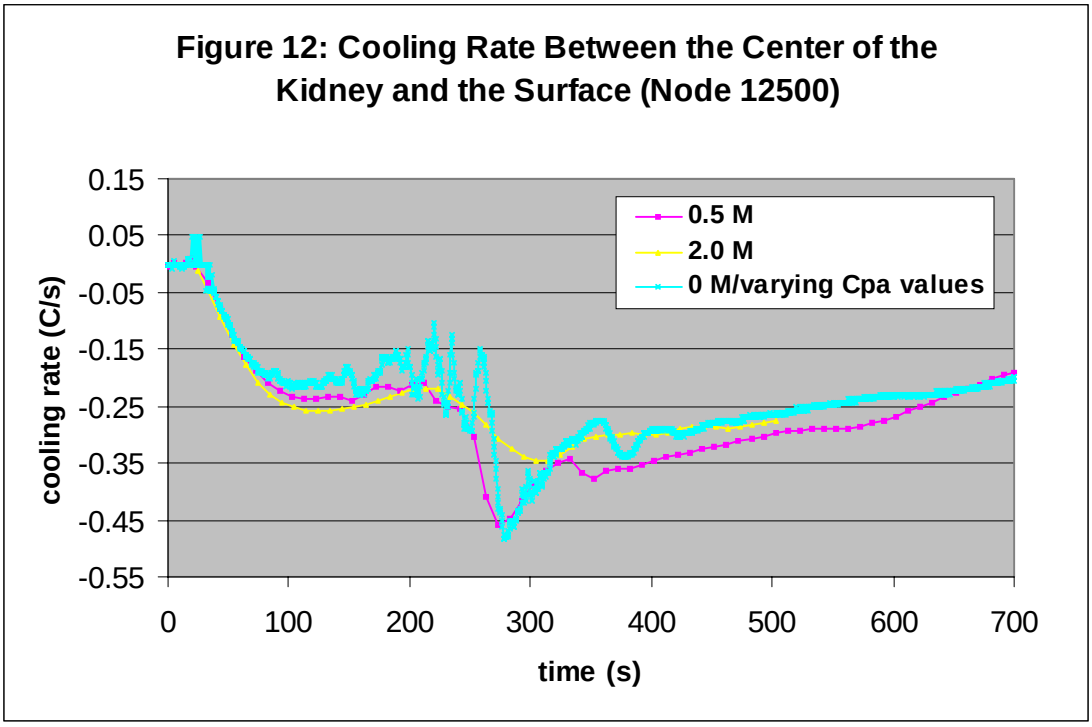

At the center of the kidney, the rapid increase in cooling rate occurs after 500 seconds, while at the intermediate point, it occurs for all concentrations of glycerol after approximately 250 seconds. From Figure 13, below, it is clear that these peaks in cooling rate (at approximately 270, 275, and 300 seconds for 0 M, 0.5 M, and 2.0 M glycerol) occur some time after the phase change would have occurred (recall from above that according to the specific heat peaks, the phase changes would have occurred at approximately –2.5, -5, and –10 C for the increasing glycerol concentrations), or at approximately 225 seconds for all three of the models.

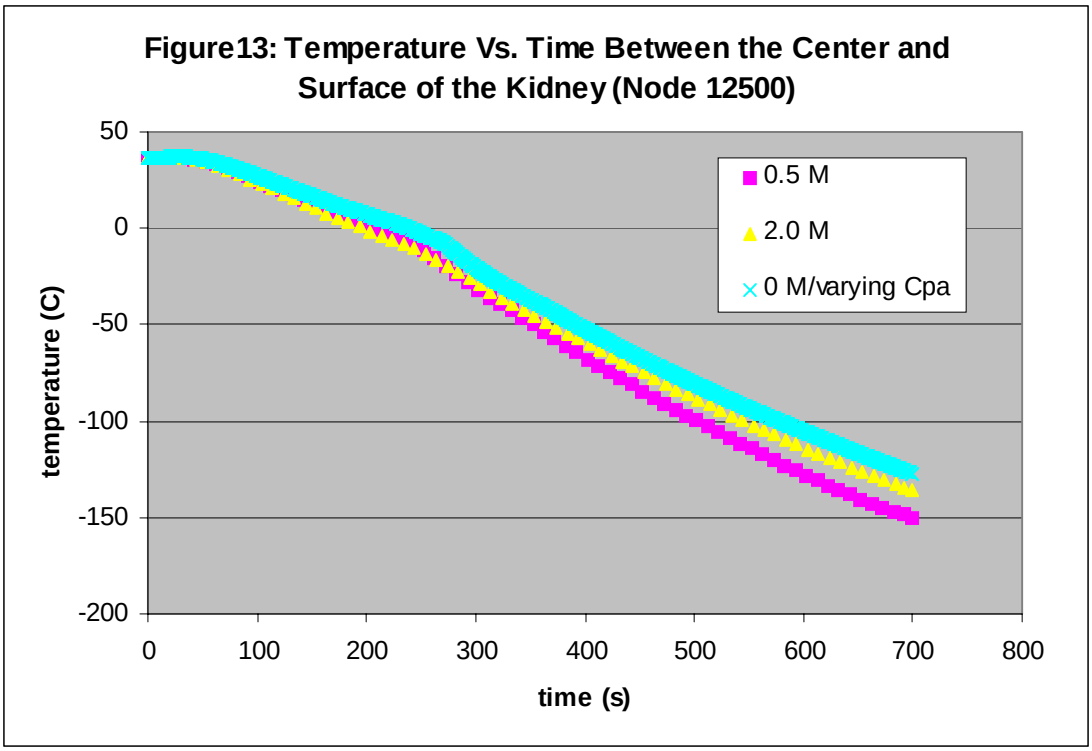

As expected, the cooling rate peaks occur earlier than they did at the center, since this node is closer to the surface. The less dramatic increase in cooling rates also corresponds to the position of this node relative to the geometry. The cells surrounding the node that are on the side nearer the surface would reach the phase change at roughly the same time, producing a cooling rate peak with the rapid conduction of heat away from the node. However, the peak is necessarily smaller than that at the center, since the simultaneous cooling occurs from only approximately half the cells that cooled the center. The less dramatic change in cooling rate due to the phase change alteration with the addition of cryoprotectant is also apparent at this point; the 2.0 M glycerol concentration gives the smallest change, with the 0 M concentration producing the largest increase. As at the center, however, the cooling rates for the 2.0 M concentration were generally larger than the other two concentrations prior to the cooling rate jump following the phase change, and the overall temperature produced during the cooling time was lower for the models using cryoprotectant.

Although much of the data is unclear, our calculations do indicate that cryoprotectants lower the apparent specific heat. The nature of vitrification is such that the intracellular fluid does not actually undergo a phase change in the usual way. Rather

than forming a crystalline solid, the viscosity of the fluid increases dramatically so that the fluid instead forms a glassy semi-solid. Thus, the addition of cryoprotectant lowers the latent heat of fusion, in a sense, by altering the phase change the fluid undergoes.

The fact that the large increases in cooling rates appear only after the phase change has occurred may be an illustration of the reason vitrification of organs cannot currently be accomplished. In the figures above it appears that, in general, the cooling rates and temperatures of the model using 2.0 M Glycerol are initially lower than those achieved using the other models. It is only later in the cooling process that the other models (namely the model without cryoprotectant) appear to have greater cooling rates. Since vitrification must occur before the fluid freezes, forming ice crystals, the process also necessarily requires that vitrification occur early in the cooling process (assuming the intracellular fluid is largely ice, it should occur before the temperature reaches 0 C). It may be that the conductivity of the kidney is simply too low to allow for effective cooling at the center, with or without cryoprotectant. Evaluation of the effects of the cryoprotectant at the intermediate point (node 12500) is useful in analyzing some of these differences. Figure 14, below, illustrates the change in cooling rate with temperature at the center of the kidney.

Figure 14: Cooling Rate with Temperature at the Center of the Kidney (Node 3942)

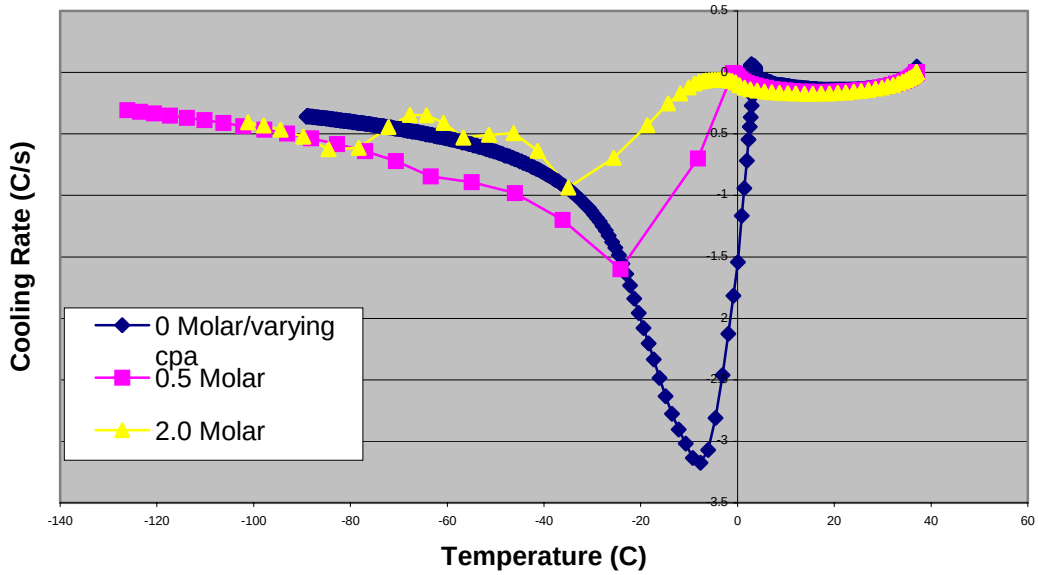

Clearly, the lowest cooling rates as the temperature reaches 0 (the expected point of phase change) are achieved using the model without cryoprotectant, which begins dropping just before 0 C, and the cooling rates using the other concentrations only drop after the temperature has already reached 0. The 2.0 M concentration model appears to begin dropping only at –10 C, after which the intracellular fluid would surely already have frozen. However, at the intermediate point, node 12500, the cooling rate patterns are significantly different, as shown in Figure 15.

Figure 15: Cooling Rates vs. Temperature Between the Center and Surface of the Kidney (Node 12500)

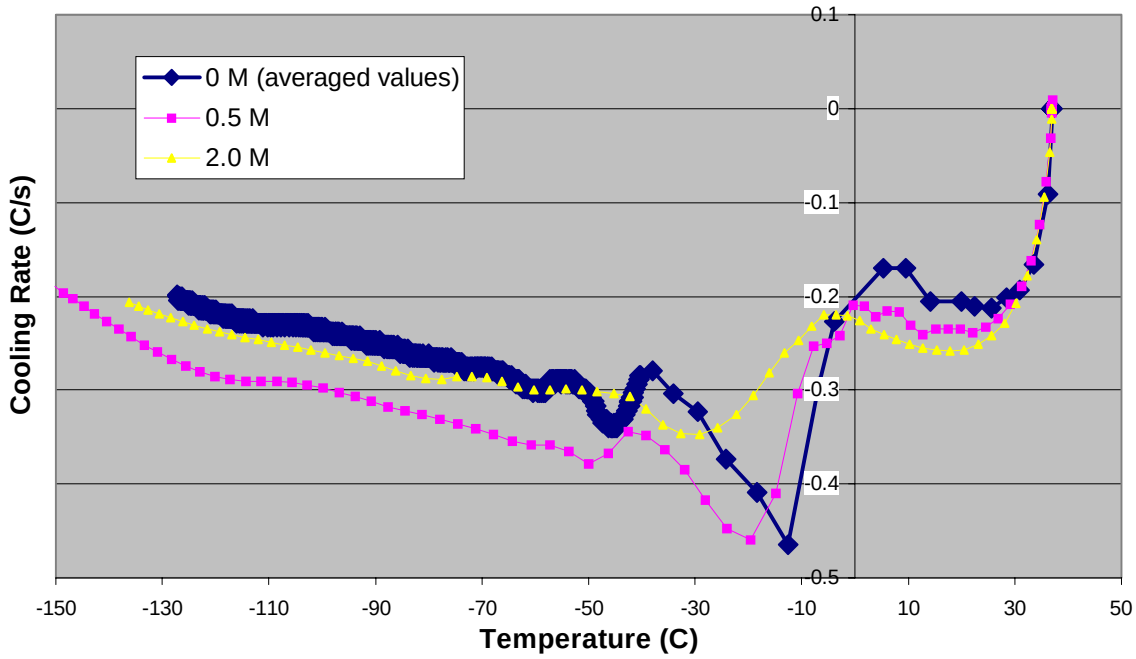

Although the data for 0 M with varying specific heat values did not entirely converge (see appendix), averaging of the data points gives a curve with a similar pattern to the other concentrations, and thus can be assumed to be a fairly accurate model of the actual cooling rate pattern. As seen above, at this point, the lowest cooling rate as the fluid reaches 0 C is given by the 2.0 M glycerol model, followed by the 0.5 M glycerol model, and finally by the model without glycerol. Although the cooling rates for the 0 M glycerol model eventually drop lower than the other two models, it is only after the fluid would likely have frozen. The 2.0 M concentration reached an estimated cooling rate of

–0.26 C/s, which corresponds to approximately 50% cell survival (Mazur, 1984). These results indicate that the cryoprotectant may be functioning as expected at areas closer to the surface, and the center of the kidney may simply be too affected by the low conductivity and heat transfer rates between the tissues to be affected by the cryoprotectant.

In addition, the effects of cryoprotectant cannot be evaluated simply based on the cooling rates. Cryoprotectants appear to affect cooling in various ways; use of 2.0 M glycerol produces an 80% cell survival rate at a cooling rate of –1.7 C/s. If 0.5 M glycerol were added, a cooling rate of ten times that would be required to achieve a cell survival rate of only 50%! Thus, cooling rate is clearly not the only factor in cell survival that is changed by the addition of a cryoprotectant.

Our hypothesis is that Fidap ^{TM} has some difficulty with convergence when the apparent specific heat values change as rapidly as they do with no cryoprotectant (figure 2). Although a more refined mesh may reduce the convergence time, it would very unfavorably increase the computation time from 4hours to 8 hours and may even cause the program to crash. Most importantly, a more refined mesh would not effect our cooling rate data, since the variation is seen is seen only in the first few seconds.

Sensitivity to Mesh Refinement and Specific Heat

Figure 16 shows a typical cooling curve for the center of the kidney, and Figure 17 shows oscillations, due to an initial coarse mesh. Further mesh refinement eliminated such oscillations. As the mesh was refined there were difficulties in running the program with the large temperature ranges mentioned. For this reason, the temperature values in the range from -196˚C to 37˚C were adjusted to a range of 0 to 1. This smaller range allowed for a more efficient program execution. This range was readjusted when creating plots from the output data. The first mesh had just over 2000 nodes, the second over 6000, and finally over 22,000 for our final mesh (Appredix A, figure A1 – A3). This final mesh eliminated the majority of convergence problems, although Fidap ^{TM} retained some difficulty with convergence when the apparent specific heat values change as rapidly as they did in the model without cryoprotectant. A fourth mesh was created with 35000

nodes, but any increase in convergence over mesh 3 (figure A4) it may have offered were considered impractical since the run time for the program was already at 4 hours for the 0 M model.

Figure 16: Time vs. Temperature at a center node

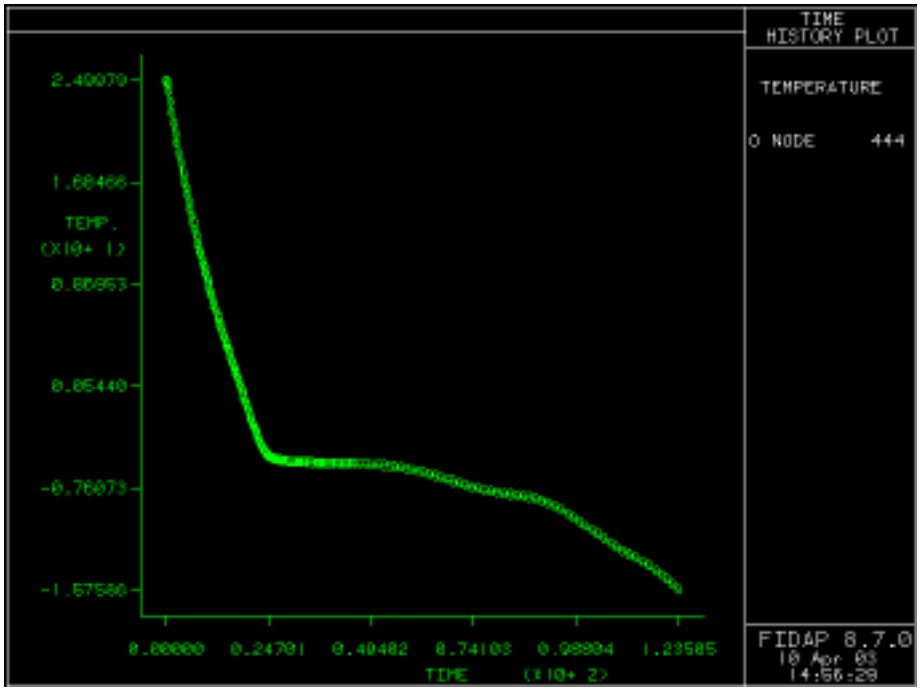

Figure 17: Time vs. Temperature at a center node

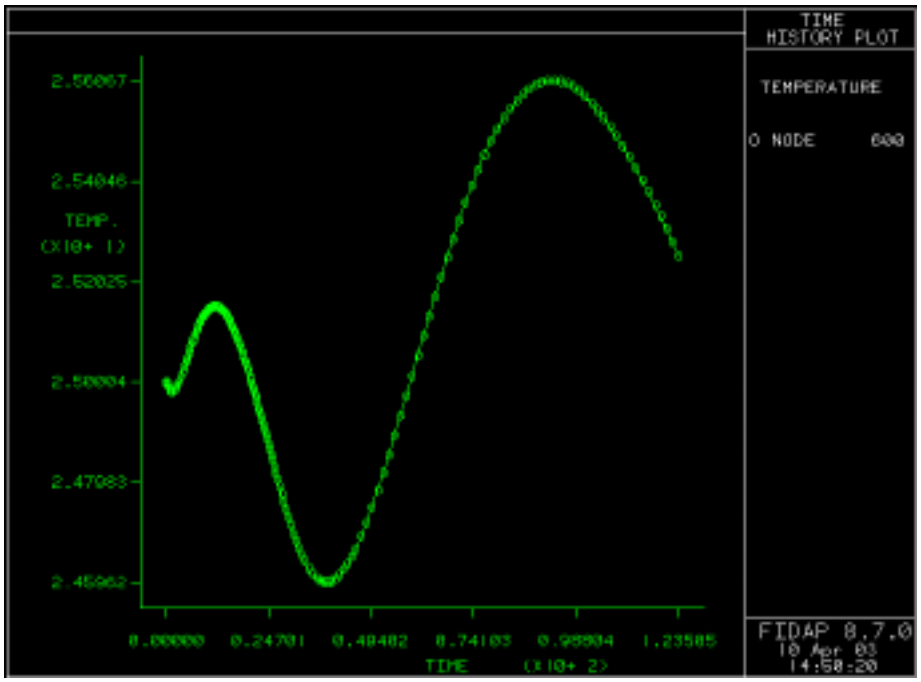

Conclusions and Design Recommendations

Given these results, complete vitrification of the kidney does not appear possible using this method. Previous research indicates, however, that even at very slow cooling rates, the addition of cryoprotectant increases the cell survival rate (Mazur, 1984). Using this data, it is estimated that for the 2.0 M model, even at the very slow cooling rates present at 400 s (the approximate time the fluid reaches the freezing point), which are estimated to be approximately –0.1 C/s, the cell survival rate would still be 40%, which, although not high enough for successful preservation, are still significant. Further addition of glycerol is not recommended, as previous studies have shown that cryoprotectants may be toxic if not removed completely. High concentrations of cryoprotectant are difficult and costly to remove entirely, and the chances that a toxic quantity of cryoprotectant would remain in the kidney increases as higher concentrations are used.

It was difficult to form any concrete conclusions about the differing effects of various concentrations of cryoprotectant in the kidney. No increase in cooling rates was observed at the center of the kidney with added cryoprotectant, but favourable increases in the cooling rates were observed at the node between the center of the kidney and the surface, indicating that the cryoprotectant may have favourable affects in areas closer to the surface.

In addition, the effects of cryoprotectant cannot be evaluated simply based on the cooling rates. Cryoprotectants appear to affect cooling in various ways; use of 2.0 M glycerol produces an 80% cell survival rate at a cooling rate of –1.7 C/s. If 0.5 M glycerol were added, a cooling rate of ten times that would be required to achieve a cell survival rate of only 50%! Thus, cooling rate is clearly not the only factor in cell survival that is changed by the addition of a cryoprotectant.

Fidap ^{TM} appears to have some difficulty with convergence when the apparent specific heat values change as rapidly as they do with no cryoprotectant (figure 2). Although a more refined mesh may reduce the convergence time, it would very unfavorably increase the computation time from 4hours to 8 hours and may even cause the program to crash. Most importantly, a more refined mesh would not effect our cooling rate data, since the variation is seen is seen only in the first few seconds.

Further research is required to determine the optimum concentration of cryoprotectant to be used in attempts to vitrify the kidney. This model agrees with previous research, supporting the hypothesis that higher concentrations of cryoprotectant may support vitrification and higher cell survival rates. However, due to the safety considerations mentioned previously, as well as the cost of removal of the cryoprotectant, it is not recommended that concentrations of cryoprotectant above 3.0 M be added.

Appendix A: Mathematical Statement of the Problem

Geometry Re-Refined ~ 22000 Nodes

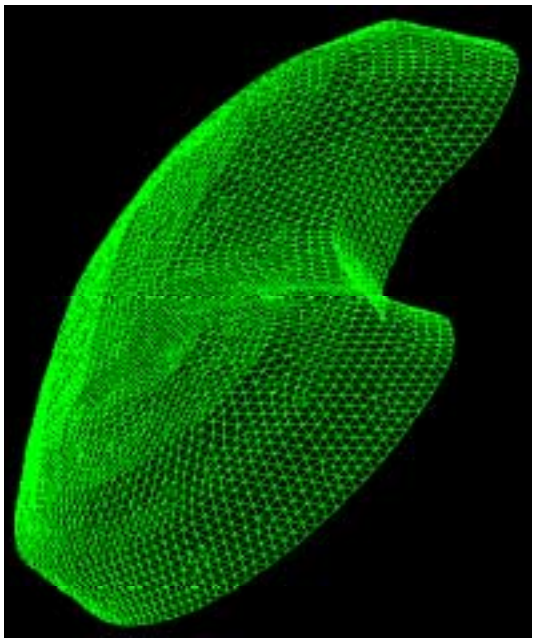

Governing Equations:

Temperature:

$$\frac{\partial T}{\partial t} = \alpha\left(\frac{\partial^2 T}{\partial x^2} + \frac{\partial^2 T}{\partial y^2} + \frac{\partial^2 T}{\partial x^2}\right)$$

Boundary and Initial Conditions:

$$\frac{\partial T}{\partial x}\Big|_{center} = 0$$

$$T_{surface} = -196$$

$$T(x, y, z, t = 0) = 37$$

(no flux through symmetry plane, constant surface temperature and isotropic initial temperature)

Properties:
See Tables 1, 2 and 3 below and graphs for varying apparent specific heat values with temperature for the different concentrations. Conductivity and density were held constant and are indicated below.

Constant Properties:
Thermal conductivity k = 0.005mW/cm K
Density = 9.9x10^-4 kg/cm^3
Specific Heat = 4200 J/kg K

Table 1: Apparent specific heat values without cryoprotectant

T (C)	Temp (no dims)	H (KJ/kg)	Cpa (kJ/Kg C)
-200	-0.017167382	14.7	2.321
-50	0.626609442	14.7	2.321
-28.9	0.717167382	14.7	2.321
-23.3	0.741201717	27.7	2.321428571
-17.8	0.764806867	42.6	2.709090909
-12.2	0.788841202	62.8	3.607142857
-9.4	0.800858369	77.7	5.321428571
-6.7	0.812446352	101.2	8.703703704
-5.6	0.817167382	115.8	13.27272727
-4.4	0.822317597	136.9	17.58333333
-3.9	0.824463519	151.6	29.4
-3.3	0.827038627	170.9	32.16666667
-2.8	0.829184549	197.2	52.6
-2.2	0.831759657	236.5	65.5
-1.7	0.833905579	278.2	83.4
-1.1	0.836480687	280	3
1.7	0.848497854	288.4	3
4.4	0.860085837	297.9	3.518518519
7.2	0.872103004	306.8	3.178571429
10	0.884120172	315.8	3.214285714
15.6	0.908154506	333.5	3.160714286
37.1	1.000429185	333.5	3.16

Table 2: Apparent specific heat values with 0.5M cryoprotectants

T (C)	Temp (no Dims)	H (KJ/kg)	1-frozen	Cpa (kJ/Kg C)
-200	-0.017167382	0	0	0
-80	0.497854077	0	0	0
-75	0.519313305	0	0	1.68
-70	0.540772532	8.415	0	1.68
-65	0.56223176	16.83	0	1.68
-60	0.583690987	25.245	0	1.68
-55	0.605150215	33.66	0	2.19
-50	0.626609442	44.595	0.01	1.95
-45	0.64806867	54.34898	0.015	1.96
-40	0.669527897	64.14244	0.02	1.97
-35	0.690987124	73.97539	0.025	3.99
-30	0.712446352	93.92783	0.07	2.30
-25	0.733905579	105.4157	0.08	2.31
-20	0.755364807	116.9825	0.09	2.33
-15	0.776824034	128.6282	0.1	5.87
-10	0.798283262	157.993	0.18	13.06
-5	0.819742489	223.2695	0.4	32.55
0	0.841201717	386.0435	1	3.26
5	0.862660944	402.356	1	3.26
10	0.884120172	418.6685	1	3.26
15	0.905579399	434.981	1	3.26

20	0.927038627	451.2935	1	3.26
25	0.948497854	467.606	1	3.26
30	0.969957082	483.9185	1	3.26
35	0.991416309	500.231	1	3.26
40	1.012875536	516.5435	1	3.26
45	1.034334764	532.856	1	3.26
50	1.055793991	549.1685	1	3.26
55	1.077253219	565.481	1	3.26
60	1.098712446	581.7935	1	9.70

Table 3: Apparent specific heat values with 2M cryoprotectants

T (C)	Temp (no dims)	H (KJ/kg)	1-frozen	Cpa (kJ/Kg C)
-200	-0.017167382	0	0	1.935
-80	0.497854077	0	0	1.935
-70	0.540772532	19.35	0.01	3.966795
-60	0.583690987	59.01795	0.1	2.34495
-50	0.626609442	82.46745	0.12	3.38454
-40	0.669527897	116.3129	0.18	2.21931
-30	0.712446352	138.506	0.19	3.495105
-20	0.755364807	173.457	0.25	8.881875
-10	0.798283262	262.2758	0.52	14.60034
0	0.841201717	408.2792	1	3.2625
10	0.884120172	440.9042	1	3.2625
20	0.927038627	473.5292	1	3.2625
30	0.969957082	506.1542	1	3.2625
40	1.012875536	538.7792	1	3.2625
50	1.055793991	571.4042	1	3.2625
60	1.098712446	604.0292	1	3.2625

Appendix B:

Problem statement:

Geometry type	3-D	The kidney is 3-D, representing one-half of a kidney
Flow regime	Incompressible	The intracellular and extracellular fluids were considered incompressible.
Simulation type	Transient	The results varied with time.
Flow type	Laminar	The flow is laminar
Convective term	Linear	No convection was considered in the problem
Fluid type	Newtonian	The fluid was assumed to behave in a Newtonian manner (it was considered to have a small percentage of solids)
Momentum equation	No momentum	There was no fluid flow through the kidney
Temperature dependence	Energy	The temperature change in the model was based on thermal conduction through the tissue and modeled using the energy equation.
Surface type	Fixed	There was no variation in the surface of the kidney (it is a solid surface)
Structural solver	No structural	No structural solver was used in the model
Elasticity remeshing	No remeshing	Fidap was not asked to remesh the kidney during processing.
Number of phases	Single phase	Only one phase change occurred over the time the temperature change was modelled
Species dependence	Species = 1	Only one species was used in the problem formulation.

Solution statement:

Solution method	Successive substitution = 10	The solution used successive substitution iterations to solve the problem, with a maximum of 10 iterations for any step.
Relaxation factor	ACCF = 0	The relaxation factor at any time was set at 0.

Time Integration:

0.5 M, 2M and constant Cp Trials

Time integration	Backward	The backwards Euler method was used for the time integration.
No. time steps	Nsteps = 1000	The total number of time integration steps was set at a maximum of 1000.
Starting time	Tstart = 0	The solution began at time t=0
Ending time	Tend = 7000	The solution ended at time t=7000
Time increment	dt = 0.01	The change in time increment was 0.01s.
Time stepping algorithm	Variable = 0.01	The time steps varied, and were determined by adherence to a tolerance level of 0.01 to the truncation errors.
No. fixed steps	Nofixed = 4	The number of fixed time increment steps at the beginning of the calculations was set to four.
Max. time increment	Dtmax = 100.0	The maximum change in time increment between successive time steps is 100.
Max Increase Factor	Incmax = 4.0	The maximum factor by which successive time steps could be increased is 4.

0 M Trial

Time integration	Backward	The backwards Euler method was used for the time integration.
No. time steps	Nsteps = 1500	The total number of time integration steps was set at a maximum of 1500 (since the maximum increase factor was decreased to 5, meaning that a large number of time steps would be required for completion of the solution
Starting time	Tstart = 0	The solution began at time t=0
Ending time	Tend = 7000	The solution ended at time t=7000
Time increment	dt = 0.01	The change in time increment was 0.01s.
Time stepping algorithm	Variable = 0.01	The time steps varied, and were determined by adherence to a tolerance level of 0.01 to the truncation errors.
No. fixed steps	Nofixed = 4	The number of fixed time increment steps at the beginning of the calculations was set to four.
Max. time increment	Dtmax = 5	The maximum change in time increment between successive time steps is 5. Attempts to run the program at higher increments produced excessive non-convergences and repeated time-step iterations when increment increases of more than 3 were attempted, due to the rapid specific heat change. The maximum increment was set to 5 to reduce non-convergence errors and repeated iterations, producing results despite a very long run-time.
Max Increase Factor	Incmax = 4.0	The maximum factor by which successive time steps could be increased is 4.

Element Mesh Plots, Refinement, and Convergence

Our mesh was refined three times to eliminate irregularities in the results (see Figures B3-B5). Figure B1 plots temperature as a function of time for node 643 using the second mesh. The temperature increases during the first 200 seconds above the initial temperature of the kidney (37 C) to approximately 40 C. Figure B2 is the same plot after the mesh refinement (using the third mesh). The temperature increase has been eliminated (the temperature reads "1" because of the scale change from –196 C - 37 C to 0 – 1; the temperature of 1 shown in Figure B2 indicates a temperature of 37 C.

Figure B1

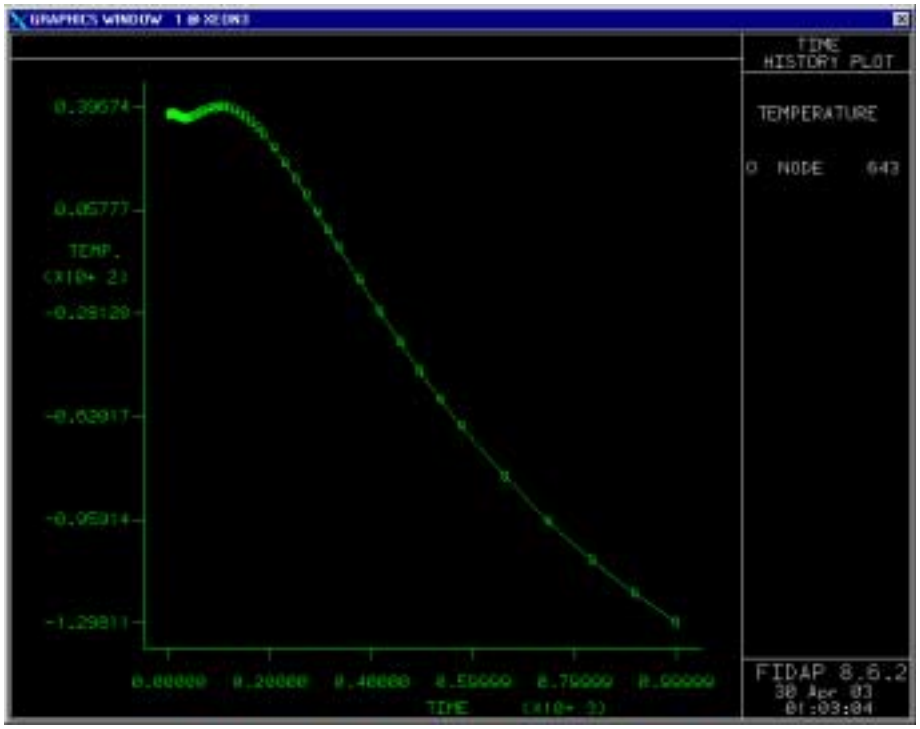

Figure B2

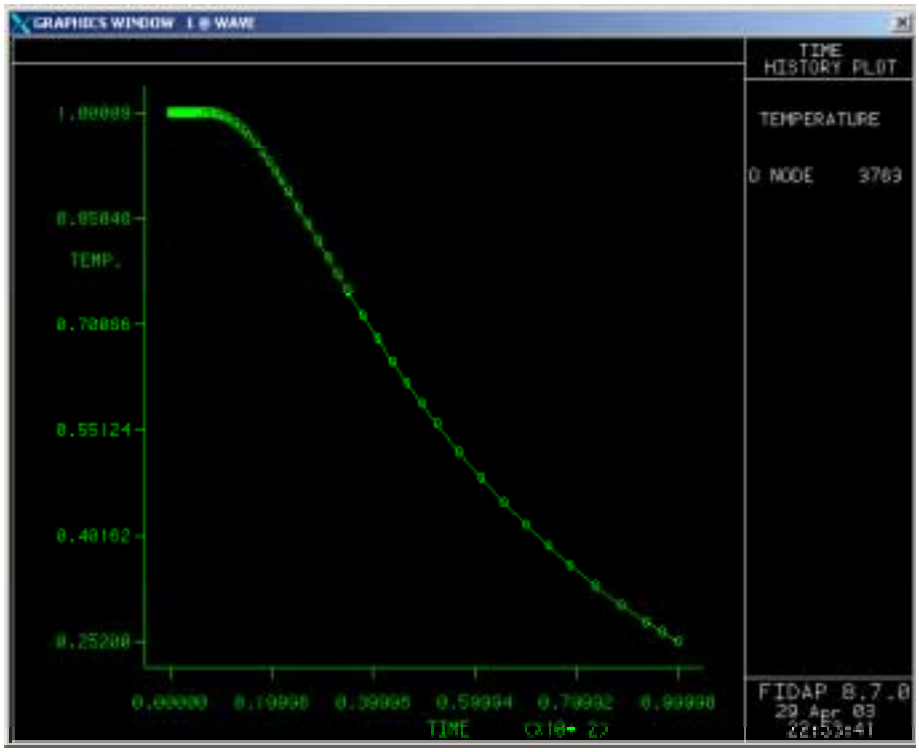

Figure B3: Geometry Unrefined ~2000 Nodes

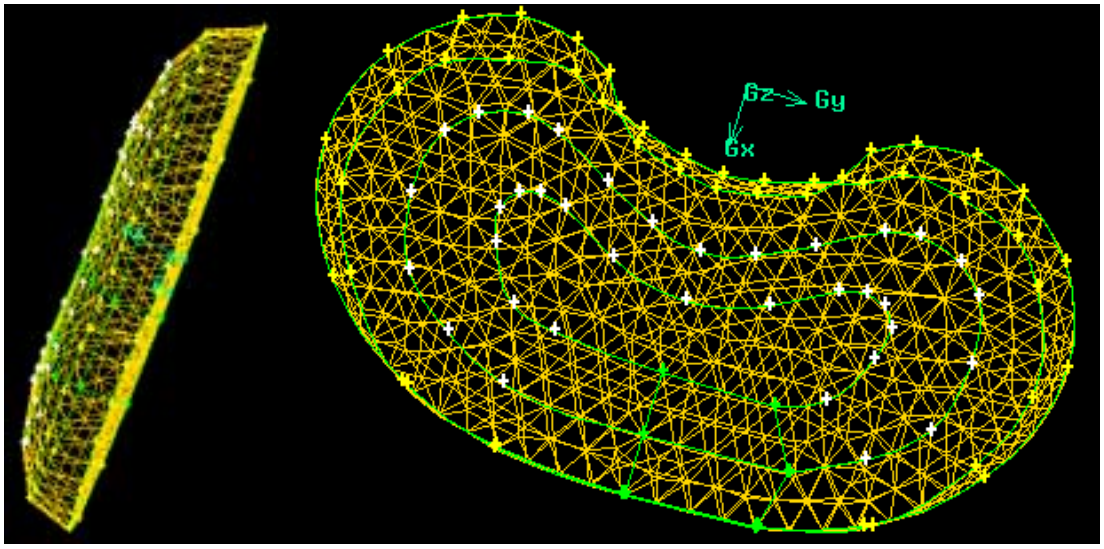

Figure B4: Geometry Refined ~ 6000 Nodes

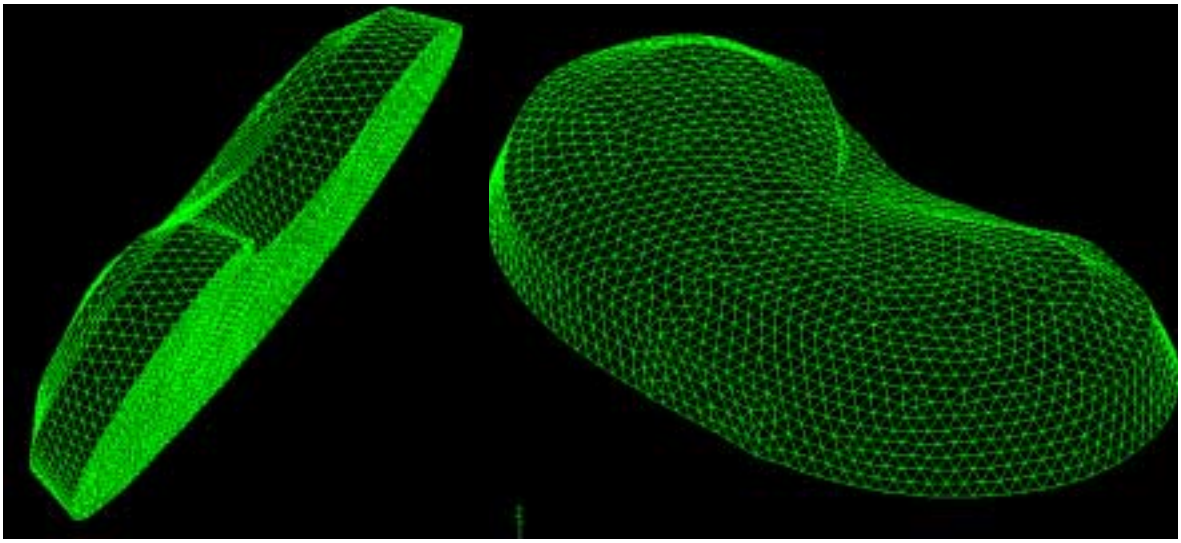

Figure B5: Geometry Re-Refined ~ 22000 Nodes

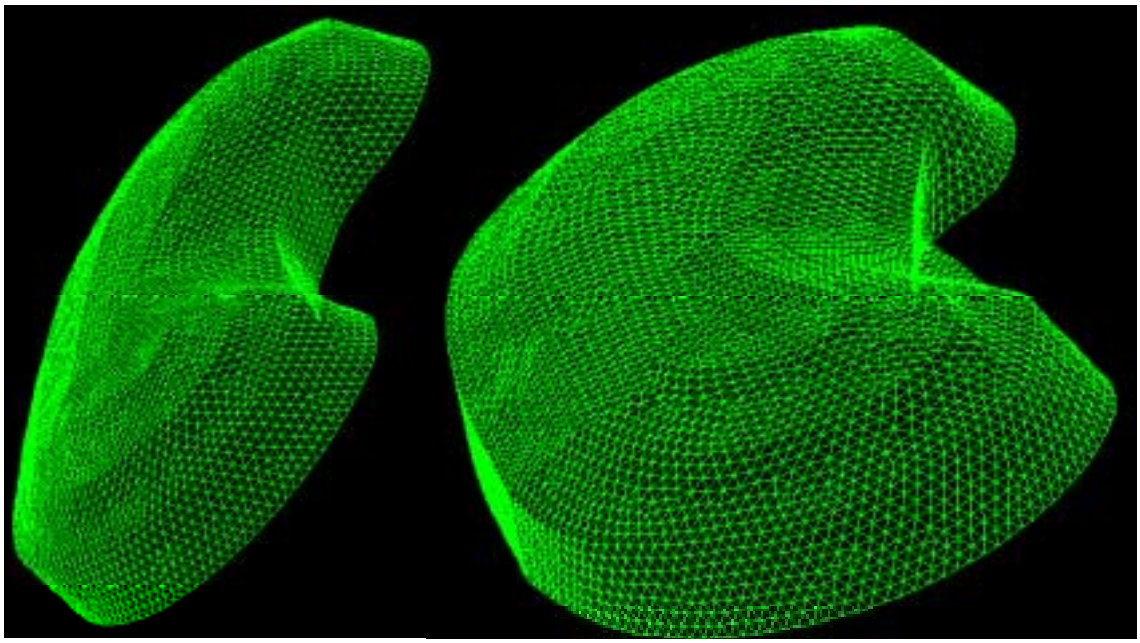

Appendix C: Special Considerations

Construction of Figure 15

Figure 15 was developed from the original data obtained for the cooling rates of the different glycerol concentration models with respect to temperature. Due to the problems with convergence in the 0 M model, the data gave a highly erratic curve, from which little could be conclusively stated. However, since the general trend of the data seemed to follow a similar pattern to the other models, an attempt to smooth the curve was made by averaging sets of the data points together to produce a smaller number of data points representing the average cooling rates and temperatures over a given time. The original graph is shown below in Figure C1, followed by the reconstructed graph, Figure C2, which was shown above as Figure 15.

Figure C1: Original Graph of Cooling Rate Vs. Temperature at Node 12500

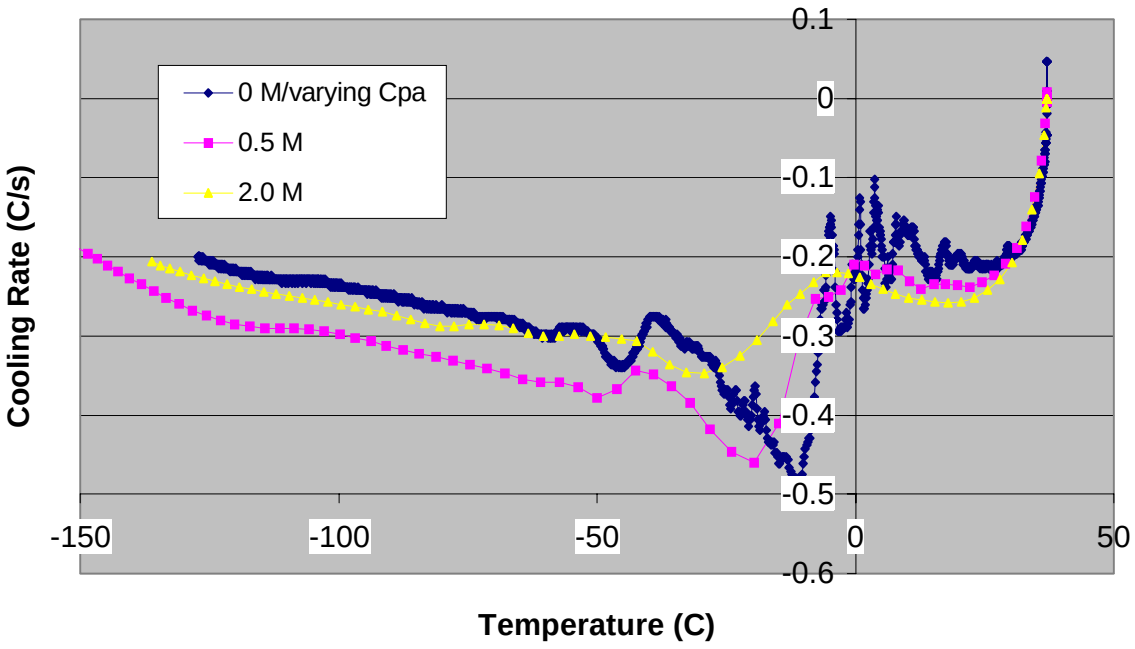

Figure C2: Averaged Cooling Rate Vs. Temperature Curve for Node 12500

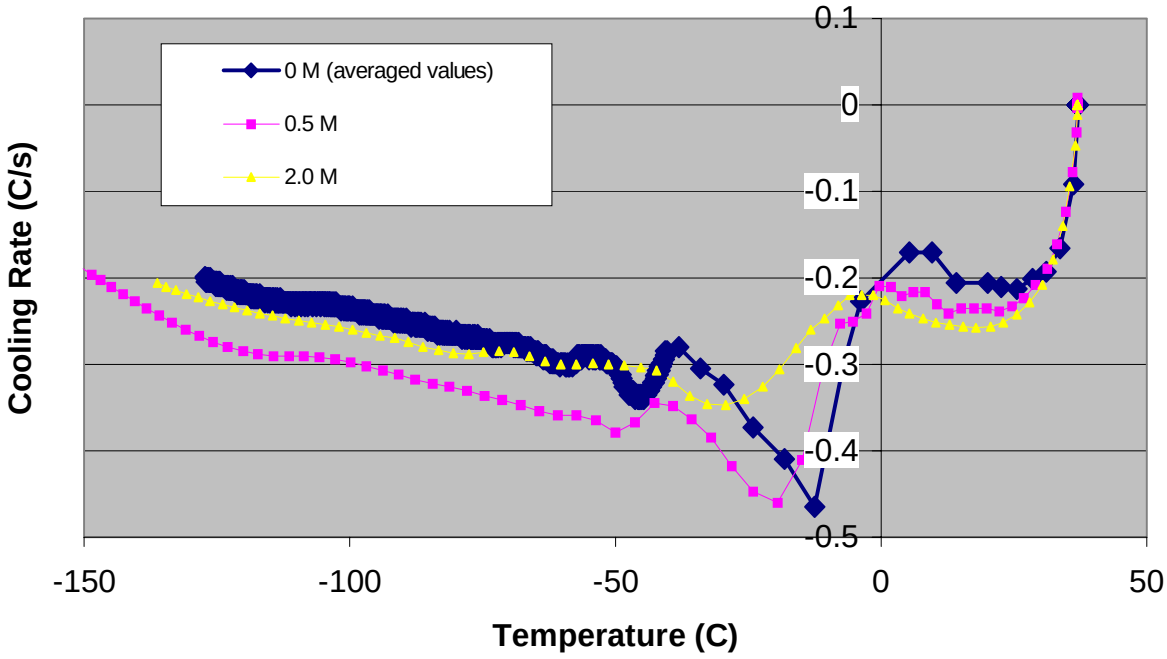

Appendix D: References

Datta, A.K. 2002. *Biological and Bioenvironmental Heat and Mass Transfer*. Marcel Dekker, Inc., New York, New York.

Datta, A.K. 2003. *Computer – Aided Engineering: Applications to Biomedical Processes*. Dept. of Biological and Environmental Engineering, Cornell University, Ithaca, New York.

Mazur, Peter. 1984. *Freezing of living cells: mechanisms and implications.* Am. J. Physiol. 247 (Cell Physiol. 16): C125-C142.

Karlsson, Jens O.M., and Toner, Mehmet. 1996. *Long-term storage of tissues by Cryopreservation: critical issues*. Biomaterials **17**, 243-256.

Fahy, G.M., MacFarlane, D.R., Angell, C.A.,and Meryman, H.T. 1984. *Vitrification as an approach to Cryopreservation*. Cryobiology **21**, 407-426.

Hayes, L.J., Diller, K.R., Chang, H.J., Lee, H.S. 1988. *Prediction of local cooling rates and cell survival during the freezing of a cylindrical specimen*. Cryobiology **25**, 67-82.

The National Institute of Health, "Treatment Methods for Kidney Failure: Kidney Transplantation". Retrieved March 11th from: http://www.niddk.nih.gov/health/kidney/pubs/kidney-failure/treatment-transplant/treatment-transplant.htm

The National Institute Diabetes & Digestive & Kidney Diseases, "Your Kidney and How They Work". Retrieved March 9th from: http://www.niddk.nih.gov/health/kidney/pubs/yourkids/index.htm